Investigation of Co-doped PZT films deposited by rf-magnetron sputtering

Felicia Gheorghiu[1,2,*], Radu Apetrei[1], Marius Dobromir[1], Adelina Ianculescu[3], Dumitru Luca[1], Liliana Mitoseriu[1,*]

[1]*Department of Physics, Al. I. Cuza Univ., 11 Bv. Carol I, 700506 Iasi, Romania*

[2]*Departament Interdisciplinary Research-RAMTECH center, Al. I. Cuza Univ., 11 Bv. Carol I, 700506 Iasi, Romania*

[3]*Polytechnics University of Bucharest, 1-7 Gh. Polizu, P.O. Box 12-134, 011061 Bucharest, Romania*

Abstract

The focus of the present paper is to describe the preparation procedure and to investigate the microstructural characteristics and the electrical properties of Co-doped PZT films deposited by rf-sputtering by using a "mixture" target system onto Au-electroded Al_2O_3 ceramic substrates. The X-ray diffraction patterns of the Co-doped PZT thin films as a function of the annealing temperature confirmed the formation of pure perovskite phase started with temperatures of 600 °C, but a perfect crystallization was achieved at a temperature of ~700 °C. The microstructures strongly depend on the thermal treatment temperature and indicated a discontinuous surface without large pores and with a bimodal grain size distribution. The XPS analysis demonstrated that the dopant element is present mainly in its Co^{2+} state. The macroscopic P(E) hysteresis loops were recorded in different locations of the films surface and demonstrated ferroelectric behaviour with a resistive leakage contribution.

Keywords: thin films, rf-sputtering, perovskite, ferroelectric behaviour

I. Introduction

In the last years, there is a great interest in preparation and investigation of different types of ferroelectric films for devices fabrication due to the search of technological applications, such as: piezoelectric devices [1,2], non-volatile random access memory devices [3], surface acoustic wave filters (SAW), micro-electromechanical systems (MEMs) and nano-electromechanical systems (NEMs) [4,5]. Among the ferroelectric materials, lead zirconate titanate (PZT) thin films are intensively studied in the literature as promising candidates for all these applications due to their quick and intense response. The large applicability of PZT family is related to the fact that possess a suitable combination of a few basic properties such as (i) high electromechanical coupling coefficient; (ii) wide range of values for the material constants (dielectric, ferroelectric, piezoelectric, piro-electric); (iii) relatively high Curie temperature, allowing a wide operating temperature range for applications and ferroelectricity at room temperature; (iv) capability to form easy solid-solutions with various compositions, thus allowing a wide range of properties values [6].

It is known that the doping can improve the electric properties of ferroelectric materials in ceramic or thin films form [7–9]. The Co-doping PZT thin films are investigated in the present paper. The Co^{2+} (ionic radius, $R = 0.75$ Å) will occupy the Pb^{2+} ($R = 1.26$ Å) sites [10] in PZT materials. The smaller Co^{2+} ions will occupy less space and this was expected to lead to enhanced ferroelectric properties. To the best of our knowledge, there are very few papers which reported properties regarding the Co-doped PZT thin films [11,12]. Consequently, it is worthy of investigating such films in order to establish and to understand the functional properties, which were not yet reported. In addition, for higher Co amounts, ferromagnetic properties at room temperature might be induced, thus turning the material into a room temperature multiferroic.

*Corresponding authors: tel: +40 232 201102 / int. 2515
e-mail: *felicia.gheorghiu@uaic.ro* (F. Gheorghiu),
e-mail: *lmtsr@uaic.ro* (L. Mitoseriu)

$PbZr_xTi_{1-x}O_3$ thin films of various compositions have been prepared using different deposition techniques, such as metal organic chemical vapour deposition (MOCVD) [13], chemical routes with metal organic precursors (sol-gel processing) [14,15] and by physical deposition routes as laser ablation [16–19] and rf-magnetron sputtering [20–22]. The method of rf-sputtering has gathered considerable interest, given the high quality of the resulted films, the relative low surface roughness, high crystallinity and easy adjustable stoichiometry [23–25]. Due to its versatility, rf-sputtering method was proposed even for mass production of PZT films [26–28]. In the present paper, the Co-doped PZT films were prepared by using a "mixture" of targets of Co small pellets onto a large ceramic target, as already proposed in the Ref. 29, where it was applied because the co-sputtering from multiple target arrangements provided the formation of special alloys in the hard disk media. The advantage of this method is that a plurality of sputtering target arrangements are disposed concentrically in one system, wherein independent magnetic fields can be generated at least partially above the respective target arrangements.

The focus of the present paper is to describe the preparation procedure and to investigate in detail (by X-ray diffraction (XRD), energy-dispersive X-ray spectroscopy (EDX), X-ray photoelectron spectroscopy (XPS), atomic force microscopy (AFM) and $P(E)$ hysteresis loops) the Co-doped PZT films deposited by rf-sputtering by using a "mixture" target system onto Au-electroded Al_2O_3 ceramic substrates.

II. Experimental details

Prior to the films deposition, Au bottom electrode was deposited onto optically polished Al_2O_3 ceramic substrates. The Co-doped PZT films were deposited by using a rf-magnetron plasma deposition facility with a 3 inches Torus magnetron (K.J. Lesker, Pittsburgh, PA, SUA) powered by a Huettinger PFG 300 RF-generator (Farmington, CT, USA). Argon (99.99% purity) was used as sputtering gas under a total pressure of 1.5×10^{-2} mbar. The films were deposited from a 3.00" diameter $\times 0.125$" thick $Pb(Zr_{0.54}Ti_{0.46})O_3$ ceramic target (Kurt J. Lesker) onto the Au/Al_2O_3 substrates (Fig. 1). The Co pellets with 8 mm diameter $\times 2$ mm thickness have been prepared by cold isostatically pressing at $p = 300$ MPa from Co powders (Aldrich 60784, purity
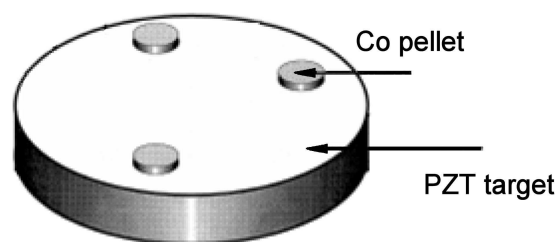

Figure 1. The "mixture" targets system

99.8%) and then radially placed in the deposition system. Distance from targets to substrate was about 6 cm, the sputtering was carried out for 300 minutes under a fixed power of 80 W. The substrate temperature was kept at the temperature of 300 °C during the entire deposition process. The amorphous as-deposited films were then subjected to a post-deposition annealing in air with a heating rate of 5 °C/min up to various temperatures in the range of 600–700 °C, with 1 hour plateau at these temperatures and then slowly cooled down to room temperature. The annealing was performed in order to allow the full crystallization into the perovskite phase.

The perovskite phase formation of the Co-doped PZT thin films after the calcination step were checked at room temperature with a Shimadzu XRD 6000 (Kyoto, Japan) diffractometer in geometry ($\theta - 2\theta$) using Ni-filtered CuKα radiation ($\lambda = 1.5418$ Å), with a scan step of 0.02° and a counting time of 1 s/step. The films microstructures were examined by using a scanning electron microscope (SEM) coupled with energy-dispersive X-ray spectroscopy (EDX) (Vega/Tescan instrument, Cranberry TWP, USA). The surface morphologies were studied by using an atomic force microscope (AFM, NanoSurf EasyScan 2 Instruments, Woburn, MA, SUA).

The XPS spectra were measured using a PHI 5000 VersaProbe XPS instrument, (Minnesota, USA). The pressure in the chamber was of 2×10^{-6} Pa and the conditions used for all of the survey scans were: energy range of 130–750 eV, 117.4 eV pass energy, 0.5 eV step size and time/step of 20 ms. XPS spectra were recorded by using PHI Summitt XPS software and the data were analysed with MultiPak Spectrum software. All the spectra were calibrated using the C 1s peak with a fixed value of 284.5 eV.

Impedance spectroscopy characterisation was performed in the frequency in the range of 20 Hz to 2 MHz by using an impedance bridge type Agilent E4980A Precision LCR Meter (Santa Clara, CA, SUA).

In order to examine the macroscopic ferroelectric behavior of the Co-doped PZT films, the polarization switching $P(E)$ characteristics were determined by using a Radiant EDU Kit system (Albuquerque, NM, SUA).

III. Results and discussion

3.1. The structural investigation

Figure 2 shows the X-ray diffraction patterns of the obtained Co-doped PZT thin films as a function of the annealing temperature. The annealing was performed in order to eliminate the pyrochlore phase and to allow the crystallization into the perovskite phase. It can be clearly seen that the formation of perovskite phase it is formed even at ~600 °C, but the highest crystallization was achieved at the higher temperatures of about 700 °C proved by the lowest intensities of the pyroclore phases, still present in this film. The pyrochlore phase amount decreases with the increasing of the annealing temper-
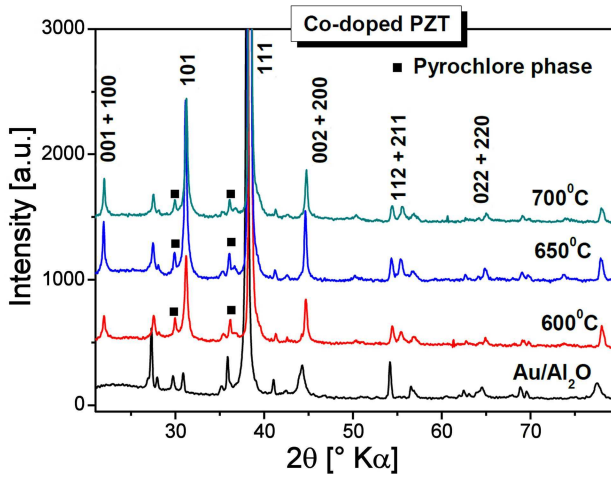
Figure 2. XRD patterns of the Co-doped PZT thin films annealed at different temperatures

ature. The XRD patterns for all the Co-doped PZT thin films still shows trace amounts of pyrochlore phases due to the PbO volatilization but clearly demonstrated the formation of the perovskite phases. The films are polycrystalline, with a strong (111) crystalline orientation. No secondary phases (as Co oxides) are identified, showing that Co entered into the perovskite cell and did not segregate as a separate phase in the film.

3.2. Surface morphology

The surface morphology of the Co-doped PZT films (Fig. 3) shows the presence of two morphological structural units observed at different magnitude levels. The microstructures clearly depend on the thermal treatment temperature and show a discontinuous surface with a bimodal size distribution, without large pores and cracks. The SEM images indicated a typical behaviour of a system with two components with different diffusion
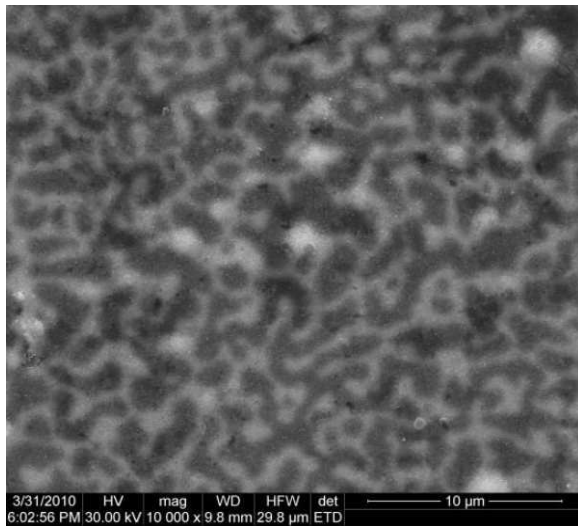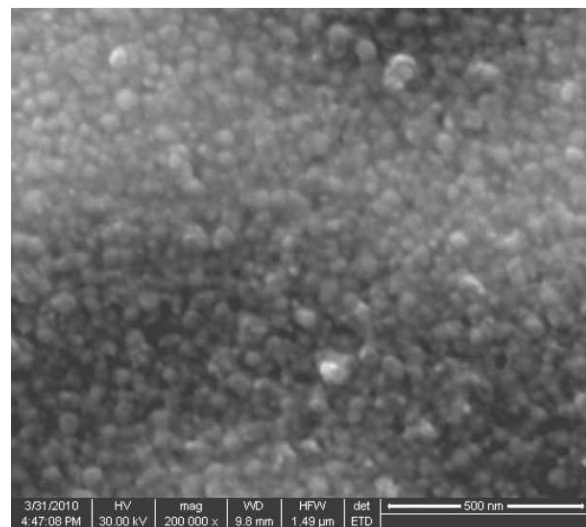

(a)
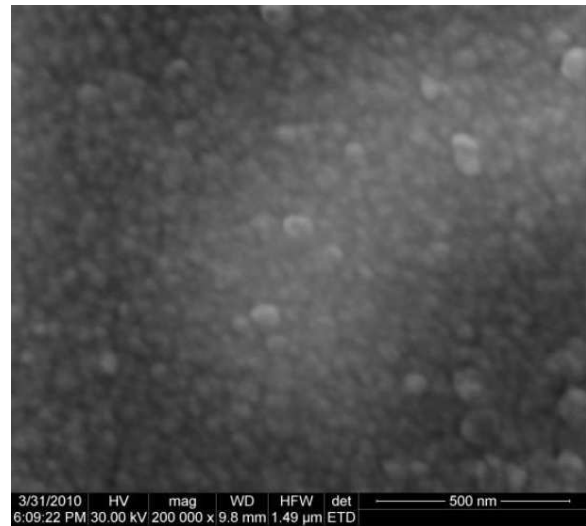
(b)
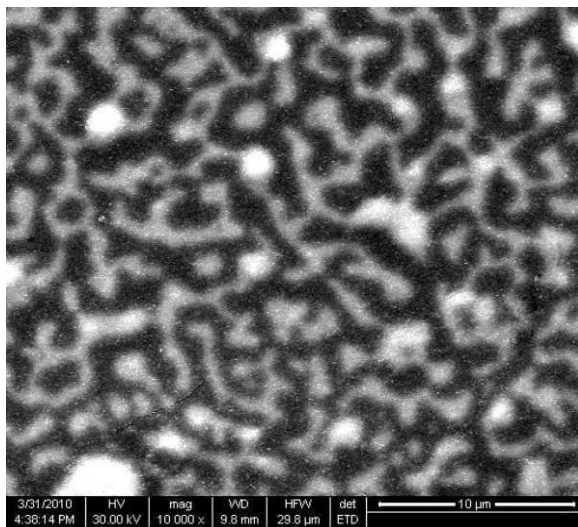
(c)

(d)

Figure 3. SEM micrographs of the rf-sputtered Co-doped PZT thin films annealed at
650 °C (×10000 (a) and ×200000 (b)) and 700 °C (×10000 (c) and ×200000 (d))
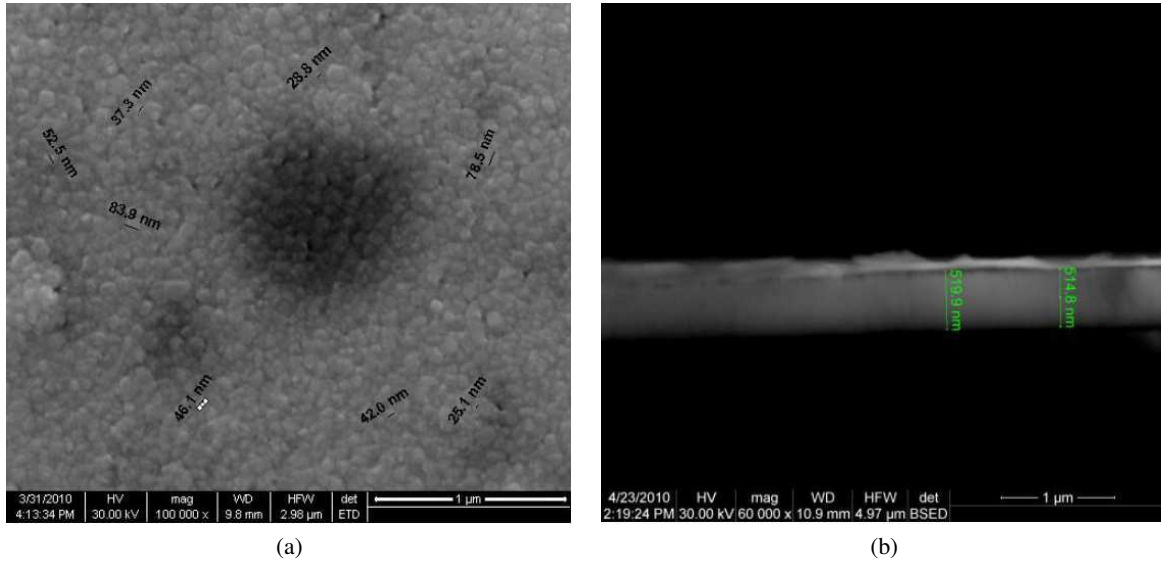
Figure 4. Surface SEM image showing the grain size in the range of (10–90) nm (a) and a cross-sectional SEM image of a 516 nm thick Co-doped PZT thin films onto Au/Al₂O₃ substrate annealed at 700 °C (b)

coefficients (long range order, LRO). These patterns are formed due to a combination of the reaction and diffusion processes giving rise to patterns of labyrinthine instabilities type [30]. These patterns can arise as a result of instabilities in the diffusion of the Co ions into the PZT thin films during non-equilibrium conditions of the deposition stage. The slowly propagating diffusion (due to the LRO) of a chemical substance has the effect over space and the local reaction. Patterns are formed by chemical kinetics of the two components (Co and PZT), which may have the role of an *activator*, *A* and *inhibitor*, *B*. Their concentrations, $A(z,t)$ and $B(z,t)$, at a specific location z on the surface determine the state (or contrast) at a given time t [31]. The way such patterns form and evolve in time is vitally important for many key technologies related to sensors, memory and recording devices.

In spite of the grain structure of the thin films deposited by rf-magnetron sputtering is not clearly visible, small grains below 40 nm beside a few larger grains of ~85 nm or agglomerations of smaller grains were observed (Fig. 4a). Fig. 4b shows the cross-sectional SEM image of the Co-PZT thin films deposited onto Au/Al₂O₃ ceramic substrates and annealed at 700 °C. The figure reveals that the thickness of the Co-doped PZT thin films is approximately 517 nm. The films annealed at temperatures of 600 °C and 650 °C have a similar thickness.

In order to examine the phase formation of the films and the homogeneity distribution of the corresponding elements onto the film surface, SEM investigations coupled with X-ray energy dispersive spectroscopy (EDX) analyses were carried out. Several regions were chosen to be analysed from the chemical point of view and thus, to estimate the local phase composition.
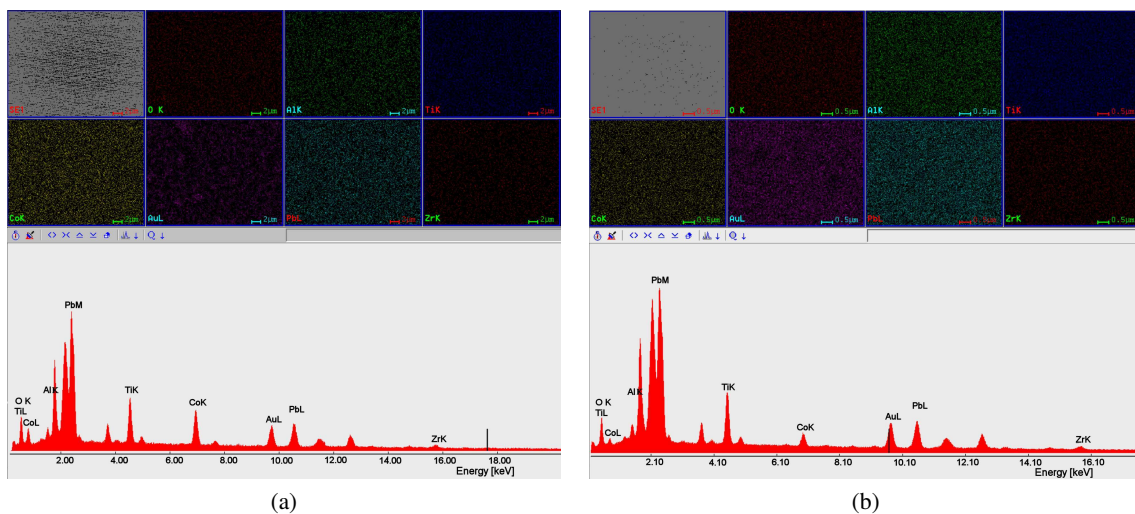

Figure 5. EDX elemental analysis for a region from the surface of Co-doped PZT thin films annealed at: a) 650 °C and b) 700 °C
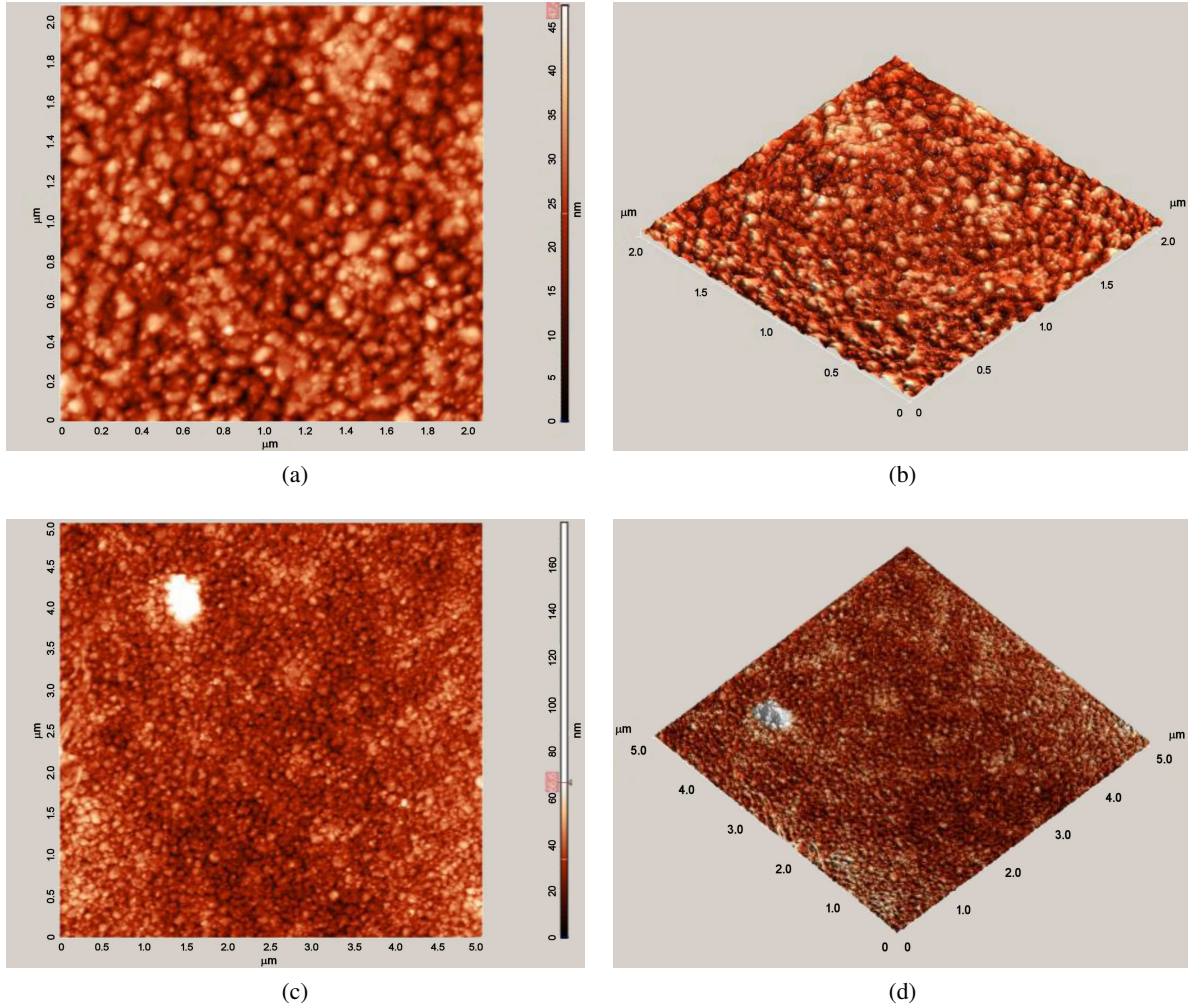
Figure 6. AFM topography of the Co-doped PZT thin films annealed at 700 °C for: a) 2D top film surface at 2 μm, b) 3D film surface at 2 μm, c) 2D top film surface 5 μm and d) 3D film surface at 5 μm

The EDX analysis performed in various films surface positions (Fig. 5) revealed that only Co, Pb, Zr, Ti and O elements are present (besides the conductive carbon traces) and they are homogeneously distributed onto the film surfaces. Therefore, no segregation of Co species as secondary phases was present, as also confirmed by the XRD analysis.

In order to better analyse the surface morphologies of the Co-doped PZT thin films, atomic force microscopy (AFM) technique was further employed. Figure 6 shows AFM images of the Co-doped PZT thin films annealing at 700 °C for different magnitudes in 2D and 3D representation. The AFM micrograph reveals that the Co-doped PZT thin film has nearly uniform grain distribution and is well crystallized and cracks free. In general, the surface is extremely dense and smooth.

Surface roughness is a commonly used measure of thin-film surface morphology and is defined as the root-mean-square (*rms*) of surface height profile as follows:

$$R_{rms} = \sqrt{\frac{\sum_{i=1}^{N}\left(h_i - h_{avg}\right)^2}{N}} \qquad (1)$$

where R_{rms} denotes surface roughness, h_i ($i = 1, 2 \ldots N$) is the surface height at the i position in the unit of layer and h_{avg} the mean value of h. The calculated R_{rms} roughness value of the Co-doped PZT films is 2.6 nm over a $2 \times 2 \, \mu m^2$ scan area, which confirms the fact that the films present a smooth and compact surface.

3.3. X-ray photoelectron spectra

In order to obtain more information about the Co-doped PZT thin film surface and to check the oxidation state of the Co dopant, a detailed X-ray Photoelectron Spectroscopy (XPS) analysis was performed. XPS depth profiling revealed that Co species are homogeneously distributed throughout the films surface. Figure 7 shows the XPS spectra of Co2p for thin films annealed at 600 °C and 700 °C. Due to higher noise, data for the films annealed at 650 °C were not good for fitting. The Co element is present mainly in the Co^{2+} state. When the films are annealed at the temperatures of 600 °C and 700 °C, the Co2p$_{3/2}$ peak is located at almost the same position of ~779.9 eV and 780.05 eV respectively, while the Co2p$_{1/2}$ is located at 795.7 eV and 796 eV. These values are in good agreement with literature reports on
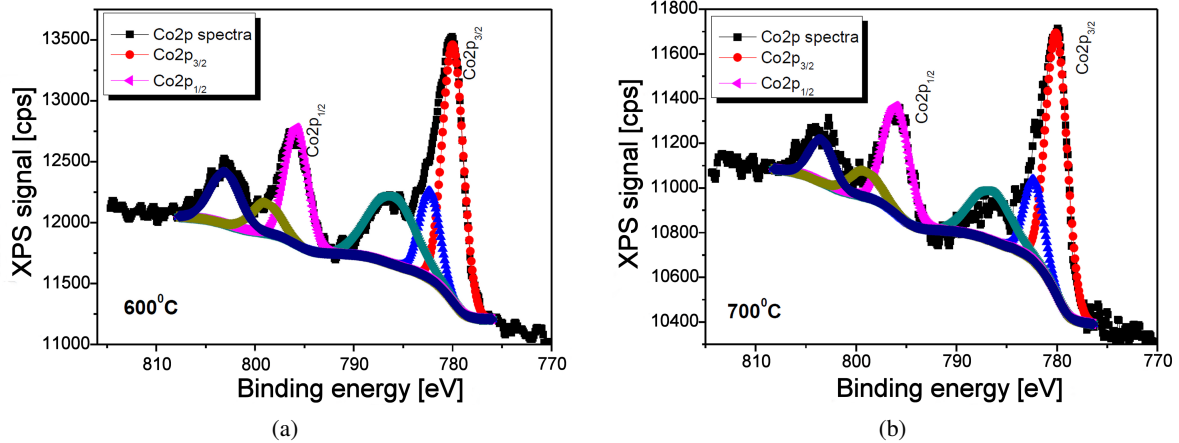
(a)

(b)

**Figure 7. Deconvolution of the XPS spectra for Co-doped PZT thin films annealed at the temperatures of:
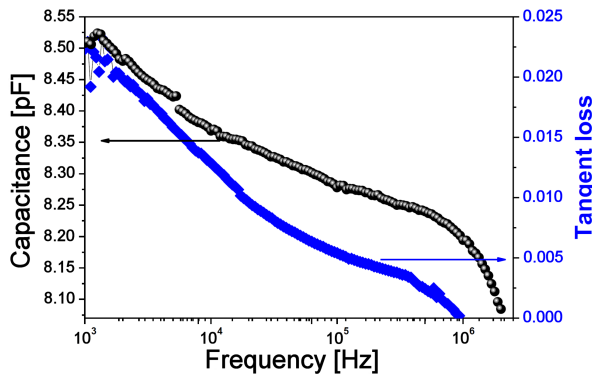a) 600 °C and b) 700 °C**

**Figure 8. Frequency dependence of the capacitance and
tangent losses for the rf-sputtered Co-doped PZT
thin films measured at room temperature**

similar systems containing Co element [32]. The rest of the peaks together with their satellites possible correspond to very small amounts of oxidized cobalt and metal cobalt (but with small amounts, below the XRD detection limit of 5%). This is the reason for which a concentration of ~67% of Co2p for both thin films annealed at 600 °C and 700 °C temperatures was obtained. In the total atomic concentrations of the film, Co^{2+} ions entered with an estimated level of about 10% in the Pb sites (generic formula $Co_{0.10}Pb_{0.90}(Zr_{0.54}Ti_{0.46})O_3$).

3.4. Dielectric and ferroelectric properties

The frequency dependence of capacitance, dielectric losses and complex impedance at room temperature for the sample annealed at 700 °C are summarized in the Fig. 8. It is seen that the measured capacitance values decreased monotonously with frequency increasing. The capacitance value for the film annealed at 700 °C was found to be around 8.5 pF at 1 kHz. An increasing of losses to 2.5% is observed at low frequencies, although in the high frequencies range the losses are below 1%. This is because at lower frequency the dielectric losses are mainly induced by leakage conduction which lead to the decrease of the dielectric losses when increasing the frequency.

The $P(E)$ hysteresis loops (Fig. 9) were measured for different locations of the films surface and at an applied voltage of 8 V amplitude. For the sample annealing at 700 °C was obtained a closed $P(E)$ loop, less affected by leakage, but still unsaturated, due to the low available voltage. Extrinsic factors as local compositional inhomogeneities and grain size, but also intrinsic random site substitutional impurities may be also responsible for such behaviour of this thin film. Although the non-linearity $P(E)$ features seem to demonstrate ferroelectric properties of this thin film, due to the resistive leakage and to the fact that the maximum field available in this experiment of $E = 150\,kV/cm$ was not enough to saturate the sample annealed at 700 °C, it is impossible to appreciate their macroscopic switching performances and it is improper to speak about true remanent polarisation and coercive field values. Better ferroelectric characterisation by PUND (positive-up/negative-down) measurements at higher voltages [33] together with local AFM piezoresponse analysis is expected to offer a better ferroelectric characterisation of these films.
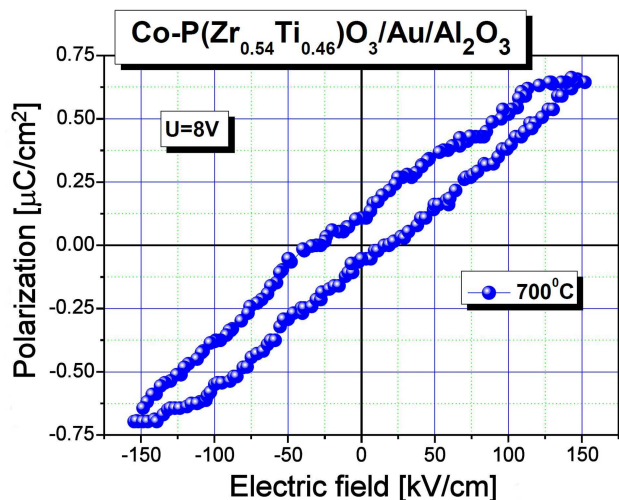

**Figure 9. Room-temperature *P(E)* hysteresis loops of
Co-doped PZT thin films at the frequency of 1 Hz**

Further investigations will be performed for a full understanding in interpreting the properties of such films and for optimising the deposition parameters in order to accomplish saturated $P(E)$ loops with high polarisation and high permittivity. In addition, magneto-optic Kerr effect (MOKE) experiments are under way in order to check the possible multiferroic behaviour of the Co-PZT films, since the magnetic measurements by a Vibrating Sample Magnetometer MicroMag™ VSM system model 3900 (Princeton Measurements Co.), did not reveal a relevant ferromagnetic behaviour, due to the lack of sensitivity for such a low level of ferromagnetic contribution.

IV. Conclusions

Co-substitutted PZT thin films with composition $Co_{0.10}Pb_{0.90}(Zr_{0.54}Ti_{0.46})O_3$ and thickness around 517 nm were deposited by rf-sputtering onto Au-electroded substrates of Al_2O_3. The formation of perovskite phase started at 600 °C, but a perfect crystallization was achieved at higher temperature of 700 °C. The films show a (111) predominant orientation. Irrespective of the annealing temperature, the films morphology present typical features resulted from the deposition of a binary system with components with dissimilar diffusion coefficients. The local EDX analysis performed in various positions of the film surface revealed that only Co, Pb, Zr, Ti and O elements are present (besides the conductive carbon traces), homogeneously distributed onto the film surface. The AFM micrographs reveals that the Co-doped PZT thin films are well crystallized and cracks free with uniform grain distributions and an R_{rms} roughness value of about 2.57 nm. The Co element is present mainly in the Co^{2+} state as it was showed by typical results of XPS Co2p spectra. The macroscopic $P(E)$ hysteresis loops were measured for different locations of the films surface and demonstrated ferroelectric properties influenced by a resistive leakage.

References

1. P. Muralt, "PZT thin films for micro sensors and actuators: a review", *J. Microeng.*, **10** (2000) 136–146.
2. D. Eichner, M. Giousouf, W. Von Munch, "Measurements on micromachined silicon accelerometers with piezoelectric sensor action", *Sensor. Actuat.*, **76** (1999) 247–252.
3. J.F. Scott, "Status report on ferroelectric memory materials", *Integr. Ferroelectr.*, **20** (1998) 15–23.
4. H.D. Chen, K.R. Udayakumar, C.J. Gaskey, L.E. Cross, "Electrical properties' maxima in thin films of the lead zirconate–lead titanate solid solution system", *Appl. Phys. Lett.*, **67** (1995) 3411–3413.
5. M. Kohli, C. Wuethrich, K. Brooks, B. Willing, M. Forster, P. Muralt, N. Setter, P. Ryser, "Pyroelectric thin-film sensor array", *Sensor. Actuat. A*, **60** (1997) 147–153.
6. R. Frunza, D. Ricinschi, F. Gheorghiu, R. Apetrei, D. Luca, L. Mitoseriu, M. Okuyama, "Preparation and characterisation of PZT films by rf-magnetron sputtering", *J. Alloy. Compd.*, **509** (2011) 6242–6246.
7. Q. Zhang, "Effects of Mn doping on the ferroelectric properties of PZT thin films", *J. Phys. D: Appl. Phys.*, **37** (2004) 98–101.
8. K.L. Yadav, "Structural, dielectric and ferroelectric properties of Y^{3+} doped PZT (65/35)", *Adv. Mater. Lett.*, **1** [3] (2010) 259–263.
9. K.W. Kwok, R.C. W. Tsang, H.L.W. Chan, C.L. Choy, "Effects of niobium doping on the piezoelectric properties of sol-gel-derived lead-zirconate-titanate films", *J. Appl. Phys.*, **95** [3] (2004) 1373–1376.
10. R.F. Zhang, H.P. Zhang, J. Ma, Y.Z. Chan, T.S. Zhang, "Effect of Y and Nb codoping on the microstructure and electrical properties of lead zirconate titanate ceramics", *Solid State Ionics*, **166** (2004) 219–223.
11. Z. Liu, Q. Liu, H. Liu, K. Yao, "Electrical properties of undoped PZT and Co-doped PCZT films deposited on ITO/glass substrates by a sol-gel method", *Phys. Stat. Solidi A*, **202** (2005) 1834–1841.
12. M. Vopsaroiu, M.G. Cain, P.D. Woolliams, P.M. Weaver, M. Stewart, C.D. Wright, Y. Tran, "Voltage control of the magnetic coercive field: Multiferroic coupling or artifact?", *J. Appl. Phys.*, **109** (2011) 066101–3.
13. M. Cerqueira, R.S. Nasar, E.R. Leite, E. Longo, J.A. Varela, "Sintering and characterization of PLZT (9/65/35)", *Ceram. Int.*, **26** [3] (2000) 231–236.
14. R. Bruchhaus, "Td19: Thin films for ferroelectric devices", *Ferroelectr.*, **133** [1-4] (1992) 73–78; Y.J. Song, Y. Zhu, S.B. Desu, "Low temperature fabrication and properties of sol-gel derived (111) oriented $Pb(Zr_{1-x}Ti_x)O_3$ thin films", *Appl. Phys. Lett.*, **72** (1998) 2686–2688.
15. A. Bhaskar, T.H. Chang, H.Y. Chang, S.Y. Cheng, "Low-temperature crystallization of sol-gel-derived lead zirconate titanate thin films using 2.45 GHz microwaves", *Thin Solid Films*, **515** (2007) 2891–2896.
16. S. Otsubo, T. Maeda, T. Minamikawa, Y. Tanezawa, A. Morimoto, T. Shimizu, "Preparation of $Pb(Zn_{0.52}Ti_{0.48})O_3$ films by laser ablation", *Jpn. J. Appl. Phys.*, **29** (1990) L133–L136.
17. H. Kidoh, T. Ogawa, H. Yashima, A. Morimoto, T. Shimizu, "Preparation of $Pb(Zr,Ti)O_3$ films on Si substrate by laser ablation", *Jpn. J.Appl. Phys.*, **31** (1992) 2965–2967.
18. P. Verardi, F. Craciun, L. Mirenghi, M. Dinescu, V. Sandu, "An XPS and XRD study of physical and chemical homogeneity of $Pb(Zr,Ti)O_3$ thin films obtained by laser deposition", *Appl. Surf. Sci.*, **138/139** (1999) 552–556.

19. M.T.N. Pham, B.A. Boukamp, H.J.M. Bouwmeester, D.H.A. Blank, "Microstructural and electrical properties of nanocomposite PZT/Pt thin films made by pulsed laser deposition", *Ceram. Int.*, **30** (2004) 1499–1503.

20. K. Iijima, I. Ueda, K. Kugimiya, "Preparation and properties of lead zirconate-titanate thin films", *Jpn. J. Appl. Phys.*, **30** [9B] (1991) 2149–2151.

21. T. Hase, T. Shiosaki, "Heteroepitaxial growth of LiTaO$_3$ single-crystal films by RF magnetron sputtering", *Jpn. J. Appl. Phys.*, **30** [9B] (1991) 2159–2162.

22. S.H. Oh, H.M. Jang, "Enhanced thermodynamic stability of tetragonal-phase field in epitaxial PZT thin films under a two-dimensional compressive stress", *Appl. Phys. Lett.*, **72** [12] (1998) 1457–1459.

23. X. Li, J. Liu, Y. Zeng, J. Liang, "Low-temperature in situ preparation of ferroelectric Pb(Zn$_{0.55}$Ti$_{0.45}$)O$_3$ thin films by reactive sputtering", *Appl. Phys. Lett.*, **63** (1993) 2345–2347.

24. T. Tunkasiri, Y.E. Qin, W. Nhuapeng, W. Thamjaree, "Structure and electrical properties of RF-sputtering deposited thin ferroelectric Pb(Zn$_{0.52}$Ti$_{0.48}$)O$_3$ films", *J. Mater. Sci. Lett.*, **19** (2000) 1913–1916.

25. T. Haccart, E. Cattan, D. Remiens, "Dielectric, ferroelectric and piezoelectric properties of sputerred PZT thin films on Si substrates: Influence of film thickness and orientation", *Semicond. Phys., Quantum Electron. Optoel.*, **5** (2002) 78–88.

26. T. Masuda, Y. Miyaguchi, M. Tanimura, Y. Nishioka, K. Suu, N. Tani, "Development of PZT sputtering method for mass-production", *Appl. Surf. Sci.*, **169-170** (2001) 539–543.

27. P. Delobelle, E. Fribourg-Blanc, O. Guillon, C. Soyer, E. Cattan, D. Remiens, "Determination by indentation method of sputtered PZT films mechanical parameters for Si-MEMs applications", *Integr. Ferroelectr.*, **69** (2005) 213–221.

28. I. Kanno, H. Kotera, T. Matsunaga, K. Wasa, "Intrinsic crystalline structure of epitaxial Pb(Zr,Ti)O$_3$ thin films", *J. Appl. Phys.*, **97** (2005) 074101.

29. T. Hata, S Kawagoe, W Zhang, K Sasaki, Y Yoshioka, "Proposal of new mixture target for PZT thin films by reactive sputtering", *Vacuum*, **51** [4] (1998) 665–671.

30. V.K. Vanag, I.R. Epstein, "Design and control of patterns in reaction-diffusion systems", *Chaos*, **18** (2008) 026107.

31. K. Leibnitz, N. Wakamiya, M. Murata, *Biologically Inspired Networking, from Cognitive Networks: Towards Self-Aware Networks*, Ed. by Q.H. Mahmoud, John Wiley & Sons Ltd., 2007.

32. X. Su, L. Wang, J. Chen, X. Wan, X. Zhang, R.P. Wang, "Role of cobalt in ZnO:Co thin films", *J. Phys. D: Appl. Phys.*, **44** (2011) 265002.

33. X.J. Lou, M. Zhang, S.A.T. Redfern, J.F. Scott, "Fatigue as a local phase decomposition: A switching-induced charge-injection model", *Phys. Rev. B*, **75** (2007) 224104.